Chapter 4: Results and Discussion

4.1 Introduction

The transition of conventional energy generation process to sustainable energy is possible with the integration of Renewable energy sources (RES). However, the transition incorporates various challenges, and one critical issue that demands attention is the Virtual Inertia problem. This chapter presents a comprehensive analysis by conducting an in-depth investigation into the Virtual Inertia issue and determining the effectiveness of the proposed method to develop the seamless integration of RES with the existing grid infrastructure. The objective of this chapter is to explore the complexities associated with virtual inertia which is a phenomenon that emerges when renewable energy, characterized by its intermittent nature, is introduced into power systems traditionally reliant on synchronous generators. The absence of physical inertia in many renewable sources poses a threat to the stability and reliability of the grid. As such, this research attempts to understand the root causes of Virtual Inertia problem and, more importantly, seeks viable solutions to mitigate its impact.

In this context, this chapter discusses various aspects of performance evaluation which serves as the empirical core of this thesis. This chapter provides the outcomes of rigorous experimentation, simulations, and analyses conducted to validate the efficacy of the proposed mitigation strategies. In the subsequent sections, the chapter provides the quantifiable results obtained from diverse scenarios and simulations. These findings not only contribute to the academic discourse surrounding renewable energy integration but also offer practical insights for the researchers, grid operators, and energy providers to effectively handle the challenges posed by Virtual Inertia.

4.2 Experimental Details

In this research, a novel virtual inertia control strategy using MPLC (Model Predictive Load Controller) controllers is proposed and implemented. A virtual inertia based droop controller is incorporated with the system. Virtual inertia is calculated using the voltage and current controller. For the controller, PWM (Pulse Width Modulation) signals are generated and the required power is sent to the inverter to obtain necessary inertia support obtained by the grid via inverter. The MPC controller is calculated by the Model Predictive Control Toolbox in MATLAB (mpc object). The reference signal is a simple sinusoidal function with a specific reference trajectory. The proposed framework is simulated by the MATLAB/Simulink environment. MATLAB provides the Control System Toolbox, which consists of a wide range of functions and tools that helps in designing, simulating, and analyzing the MPLC controller for addressing the problem of virtual inertia. The functions in MATLAB are used for creating state-space models, transfer functions, and discrete-time models, which are crucial for controller design and simulation. In the MATLAB platform, the simulation loop updates the controller at each time step and applies the calculated control input to the system.

The simulation parameters used for the analysis are tabulated in table 1.

Table 2. Simulation parameters

variables	Values
Outcomevoltage of PV system	300 V
Outcome power of PV	10 kW
Operating frequency	60 Hz
Outcomevoltage of wind turbine	300 V
Outcome power of wind turbine	3 kW

Through the integration of controllers into the proposed system model, variables are chosen to be appropriate for control systems with closed loops. This aids in researching the MPLC controller's changing actions over a given time frame. The system behavior and controller setting can be changed with the aid of the interactive simulations, which is essential for fine-tuning t2226he configurations utilized in the MPLC design. Getting an ideal frequency assessment of stability for the grid-connected RES system is the primary goal of the study. This section presents the findings from the computer simulation analysis.

4.3 Performance Analysis

The electricity produced by various sources of clean energy, such as a PV (Photovoltaic) system and an atmospheric energy system, is taken into consideration for assessing effectiveness. A most Power Point Tracking (MPPT) method is used to find and preserve the location on the surface of the solar panels where it provides the most possible power in order to maximize the electricity from the PV resources. This is crucial since a photovoltaic panel's power production fluctuates depending on the humidity, temperature, shade, and strength of the sun. As seen in the numbers below, the MPPT method uses solar energy that produces about 10 KW of power, while turbines powered by winds provide 3 KW of power.

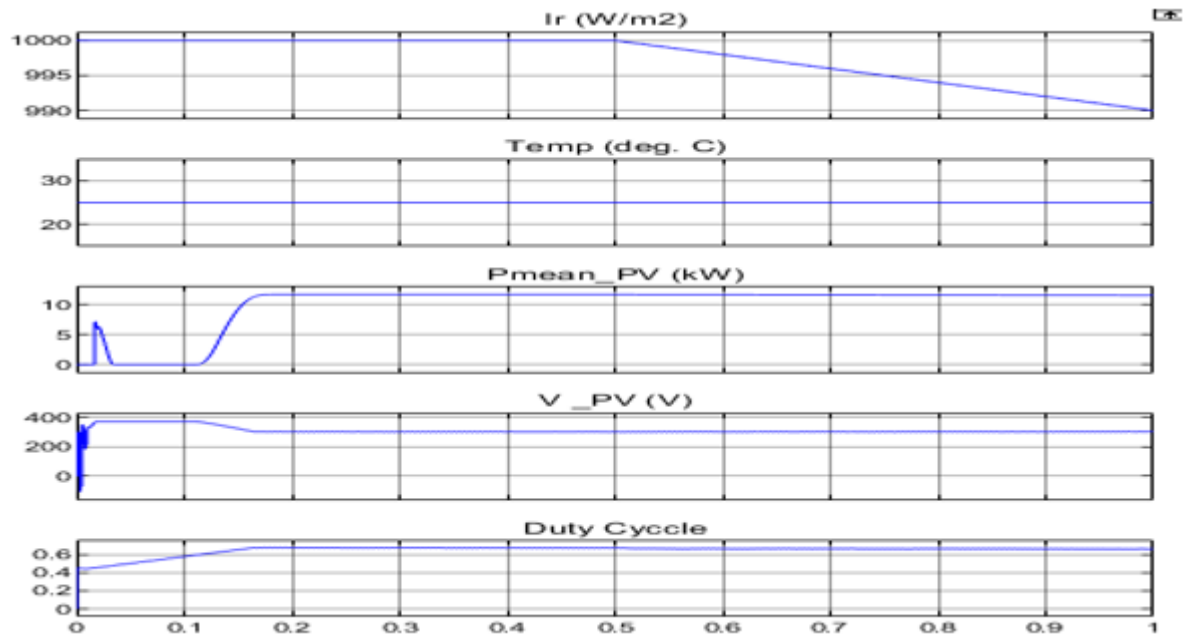

Figure 4.1 Output waveforms of solar PV system

The graph illustrated in figure 4.1 the MPPT algorithm enabled the PV system to generate a maximum solar irradiance of 1000 W/m^2. This states that under ideal conditions, the PV system is receiving sunlight at a rate of 1000 W/m^2. This value represents the intensity of solar radiation reaching the surface of the solar panels. Under this irradiance level, a well-designed PV system should produce its maximum power output. The actual power output will depend on the efficiency of the solar panels, temperature, shading, and other factors. On the other hand, The system's operating temperature achieves an elevated level of 300 V, and the mean power value displays steady state effectiveness. Figure 4.2 displays what the system's emission pattern.

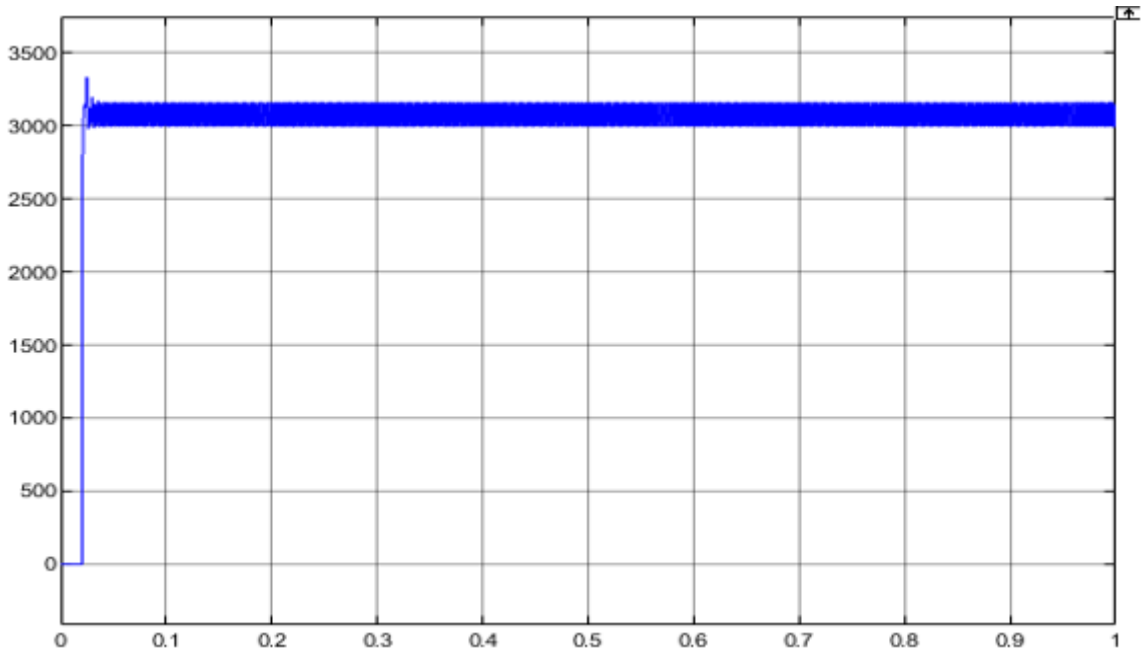

Figure 4.2 Output of the wind turbine

This research employs a nine level multi power level inverter for achieving the effective integration with the grid system. The output of the inverter is shown in figure 4.3.

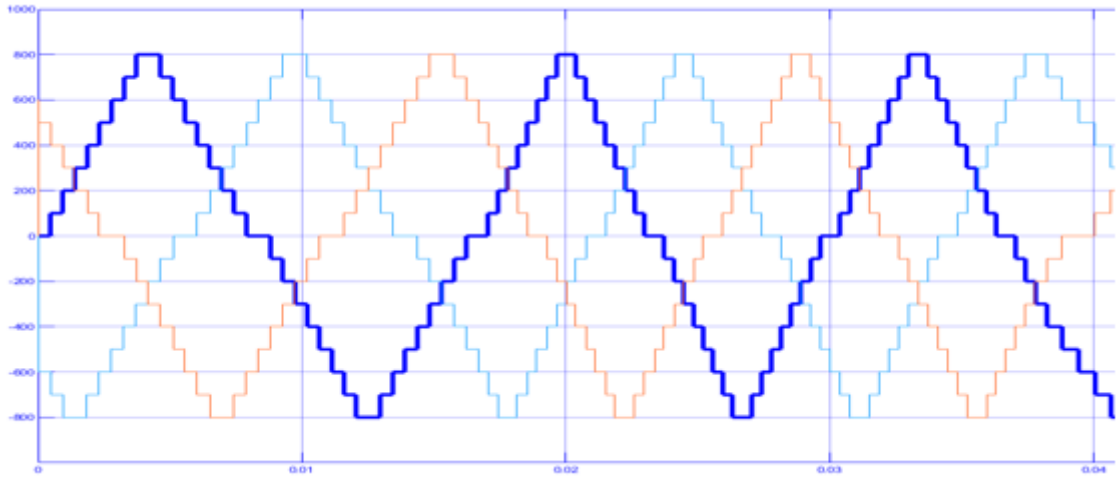

Figure 4.3 outcome of the nine level multi power inverter

The adoption of multiple power levels significantly improved the quality of power and reduced harmonic distortion as observed from figure 4.3. The additional power levels allow for the synthesis of a more sinusoidal output waveform, reducing harmonic distortion. This is particularly important for avoiding interference with other connected equipment and ensuring efficient power transfer to the grid. The high power quality outcome without major harmonic distortion makes it suitable for addressing the problem caused due to virtual inertia which is crucial in applications such as grid-tied renewable energy systems. In addition, In order to examine how the system behaves under unexpected connectivity loads, the VIC's performance with the MPLC controller is assessed. Two scenarios are run in the simulation: (i) abrupt 75 kW load connections, and (ii) sudden 75 kW load disconnections.

4.3.1 For sudden connecting loads

The performance of a power grid can be affected by sudden changes in load conditions, and the impact largely depends on the magnitude, duration, and nature of the load change. Sudden connecting load conditions, for example the abrupt connection or disconnection of a large load, can lead to several consequences such as dynamic voltage fluctuations, variation in the operating frequency, voltage stability issues, and deterioration in the power quality. Rapid changes in load can cause voltage fluctuations in the power grid. If the load is suddenly connected, it can lead to a transient voltage drop. Conversely, if the load is suddenly disconnected, it can result in a transient voltage rise

Figure 4.3 illustrates the addition of a 75 kW demand to the grid for unexpected connection loads, and figure 4.4 displays the inverter's generated current.

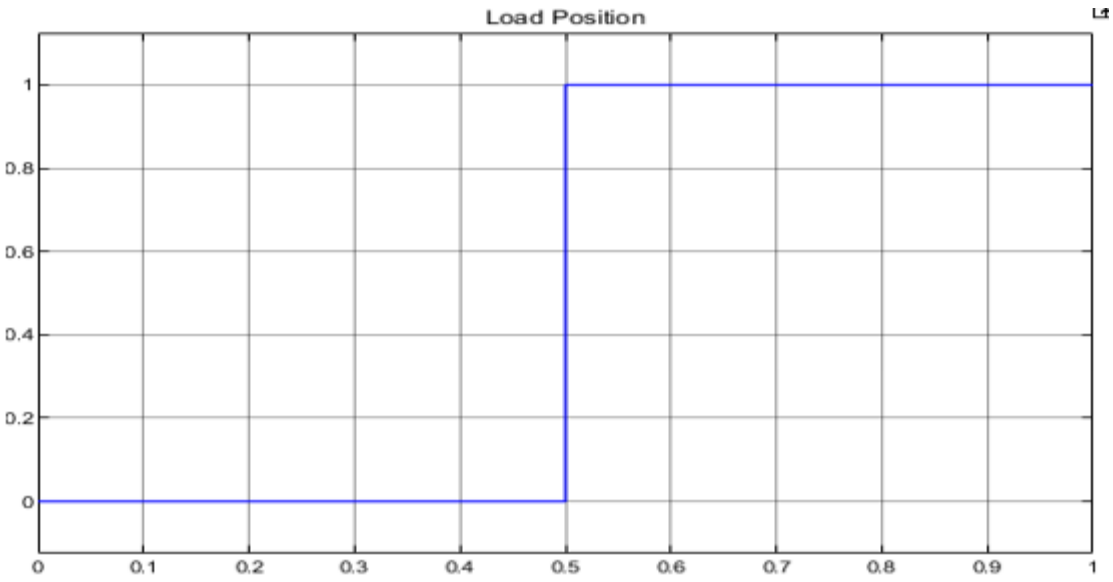

Figure 4.4 load location with an abrupt change in the connected load

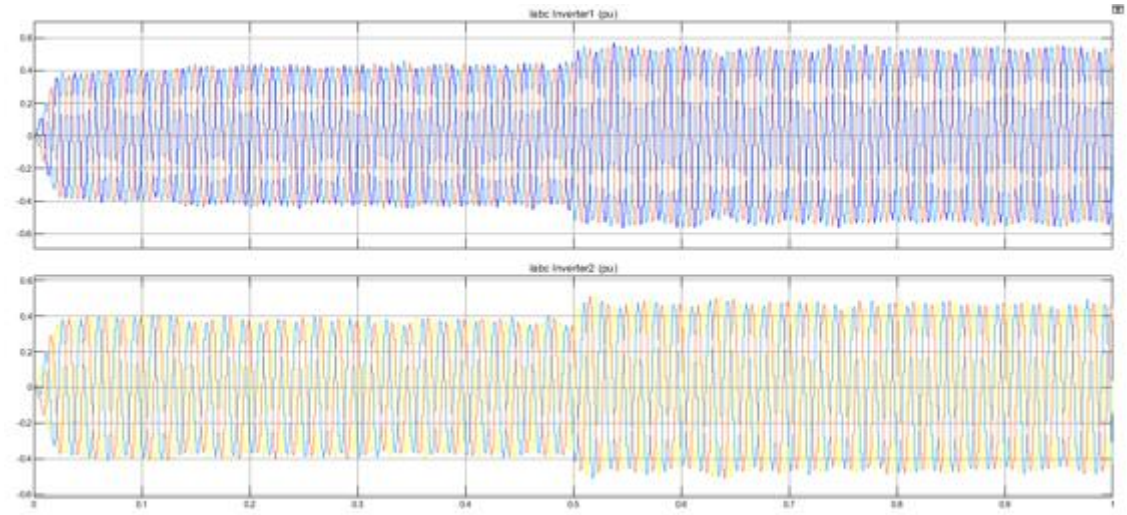

Figure 4.5 Difference of inverter outcome current with unexpected modification in the load

When a new load is suddenly connected to the grid, there is an initial surge in current as the system responds to the increased demand. This surge, often referred to as a transient overcurrent, can be higher than the steady-state current and is usually temporary. As observed from the output graph shown in figure 4.5, the sudden demand in the load is high and hence the inverter output current increases from 0.4 p.u. Hence, the proposed controller enables the exchange of power between grid and the inverter such that the inverter supplies required power to the grid whenever required through RESs. The power supplied to the grid is demonstrated in figure 4.6.

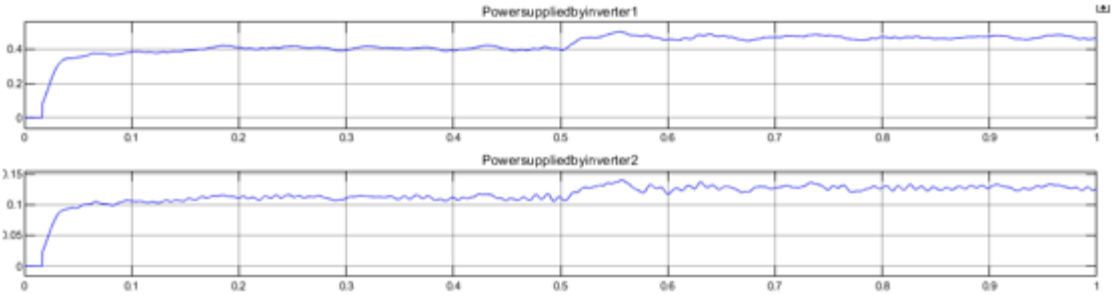

Figure 4.6 Power supplied by the inverter to grid through unexpected connection of loads

When the load is added into the grid, initially, there is often a surge in the power supplied by the inverter. This surge is a result of the inverter responding to the sudden increase in load demand. The inverter attempts to satisfy the new load requirements by supplying additional power to the grid. The inverter may experience a transient overpower condition during the initial moments of load connection. This is characterized by a long time duration during which the inverter output power exceeds its rated capacity as it compensates for the sudden load change. The inverter control system responds to the sudden load connection by adjusting the output voltage and frequency. In grid-tied inverters, preserving voltage and frequency within acceptable limits is crucial for synchronization with the grid. As observed from figure 4.6 there is a moderate variation in the power supplied as and this is due constant perturbations in the power supplied caused by the unexpected variations in the load. The change in the output frequency due to the sudden connecting load is shown in figure 4.7.

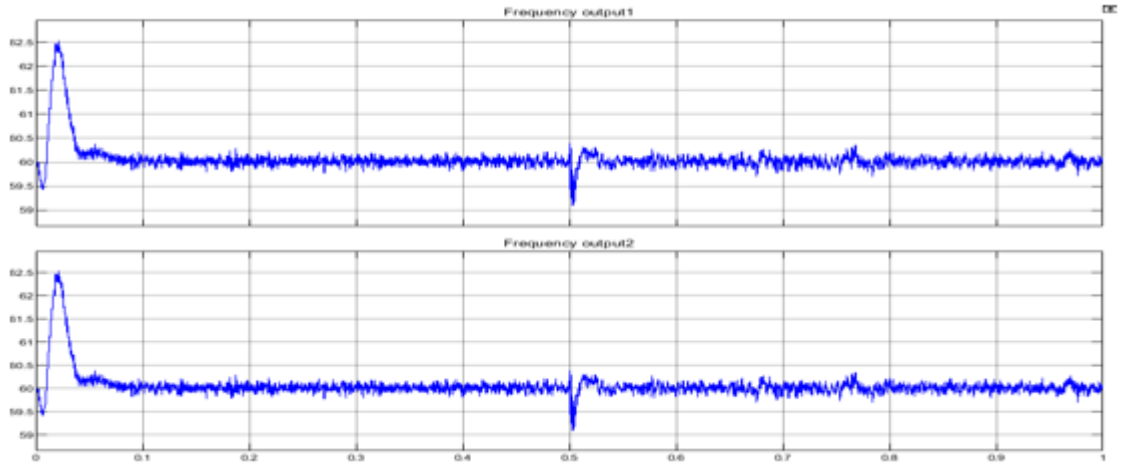

Figure 4.7 Frequency output for sudden connecting loads

Under sudden load conditions when an additional load is connected to the power grid, it can have an impact on the frequency of the grid. The frequency of the power system is one of the crucial parameters that maintains the balance between energy generation and consumption. The most common effect of a sudden load connection is a temporary drop in grid frequency. When a new load is connected, there is an immediate increase in the demand for electrical power. If the system is not able to instantaneously match the increased demand with an equivalent increase in generation, the frequency drops. This is because the energy generation performance of the generators reduces due to the additional load. The grid frequency represents the balance

between the total power generated and the total power consumed. If the sudden load connection results in an imbalance where demand exceeds supply, the frequency drops. Conversely, if there is excess generation capacity, the frequency may rise. In this case, the output frequency of the grid system decreases up to 59.2Hz and again maintains the same frequency as shown in figure 4.7. It can be inferred that the proposed approach maintains an almost stable frequency irrespective of the changes in the load position. This ensures the stability of the grid system. The variations in the grid performance for sudden disconnecting load condition is discussed in the next section.

4.3.2 For sudden disconnecting loads

When a sudden load is disconnected from the power grid, it can have various effects on the performance of the grid. The impact depends on the magnitude of the load disconnection, the available generation capacity, the response of control systems, and the overall stability of the power system. There are several aspects to be considered regarding the performance of the grid under sudden load disconnection such as increase in the operating frequency, voltage rise, instability issues, and grid resilience. For sudden disconnecting loads a 75 kW load is disconnected from the grid as shown in figure 4.8 and the outcome present of the inverter is shown in figure 4.8.

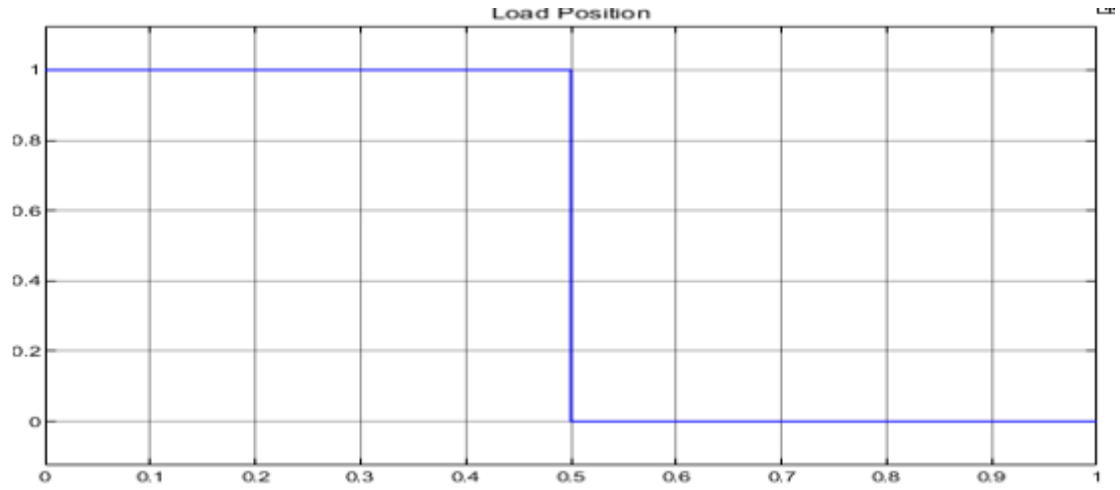

Figure 4.8 Load position with unexpected difference after disconnecting the load

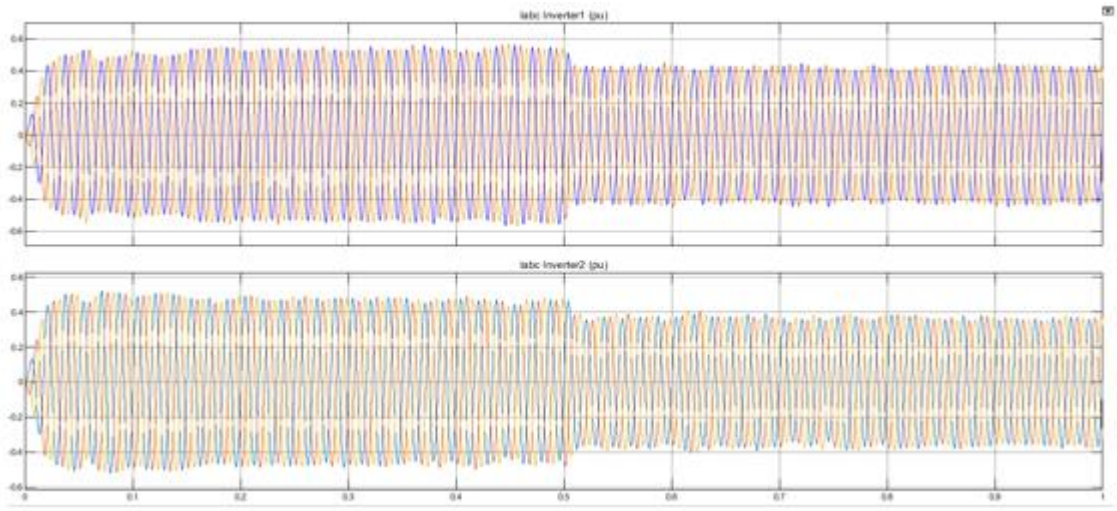

Figure 4.9 Variation of inverter output current after disconnecting the load

When a sudden load is disconnected from the power grid, the output current of the grid experiences changes, particularly in response to the decrease in demand. The behavior of the output current depends on the characteristics of the power system. Initially, there might be a transient surge in the grid current immediately after the load is disconnected. This is because the generators, which were previously supplying power to the disconnected load, experience a sudden reduction in load demand. As observed from the output graph presented in figure 4.9, the sudden disconnection of load reduces the inverter outcome current from 0.5 p.u to 0.4 p.u. In this case, the power from the inverter decreases based on the load demand and power absorbed by the super capacitor. As a result the inertia reduces. The power supplied to the grid is illustrated in figure 4.10.

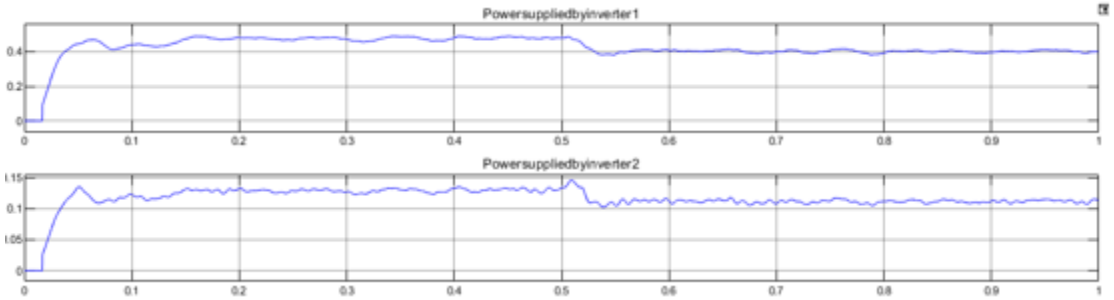

Figure 4.10 Power supplied by the inverter to grid after disconnecting the load

The operation of the inverter is majorly influenced by its control strategy especially with regards to the characteristics of the power system, and the specific features of the inverter such as voltage rise, frequency rise and power surplus. Under sudden disconnection of load from the grid, there is a variation in the power supplied as observed from figure 4.10. In this case, the power supplied is incorporated with constant perturbations and this is due to the variation in the load. The corresponding change in the output frequency is shown in figure 4.11.

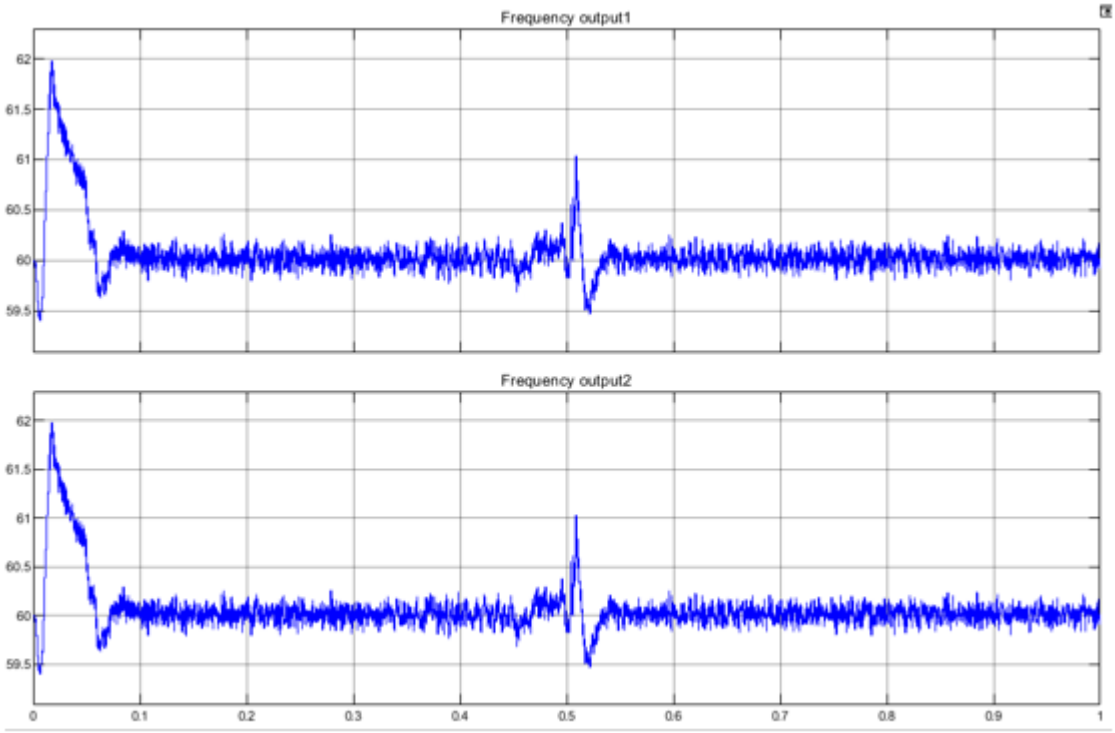

Figure 4.11 Frequency output after disconnecting the load

When a sudden load is disconnected from the power grid, the frequency of the grid tends to increase. Sudden load disconnection leads to an immediate reduction in the demand for electrical power. With less demand, the generators connected to the grid experience a surplus of power production and when the load decreases, the rotating masses of the generators increase which in turn increase the grid frequency. As shown in figure 4.11, the output frequency of the grid system increases from 59.5 Hz to 61 Hz. Further, the same frequency is maintained at a constant value. The rate of changes can stabilize after enduring brief fluctuations, even in the event of an abrupt shift in the load. Figures 4.12 show the performance of the suggested method for abrupt connection load circumstances in conjunction with and without MPLC.

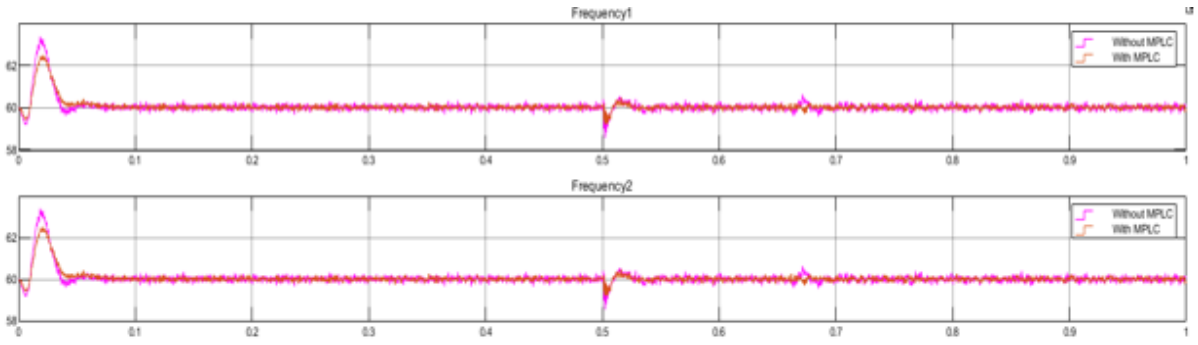

Figure 4.12 Frequency response for sudden connecting load

The proposed MPLC controllers implement active power control strategies on generators to adjust the output in real-time. The metastatic pulmonary system compels the engines to lower their active electrical output in the event of an abrupt load disconnection in order to avoid

frequency fluctuations. Figure 4.13 shows the effectiveness of the recommended approach both with and without MPLC for unexpected load reduction.

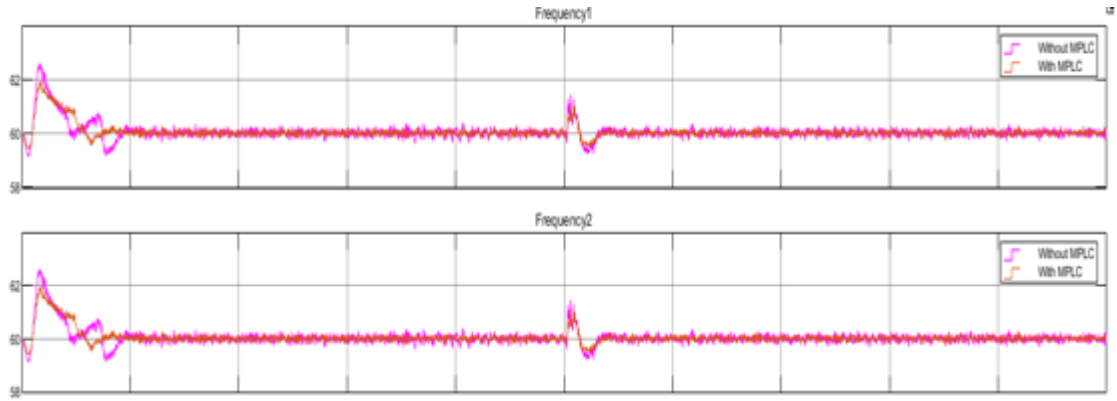

Figure 4.13 Frequency response for sudden disconnection of load

It can be observed from figure 4.13, the proposed MPLC controller is highly successful in maintaining the stable frequency response under varying load conditions. The variation of frequency is observed to be at 58.5 Hz without the MPLC strategy. In comparison to the inertia period, the variation in the frequency is greater than 1 Hz. Correspondingly, without MPLC, the frequency changes to below 59 Hz during the inertia period and the frequency variation is controlled below 0.8 Hz. Results of the simulation analysis show that MPLC is highly effective in controlling the frequency and thereby ensures that the grid frequency remains within acceptable limits. This factor enables generators to calibrate the outputs in real-time. The effective control mechanism also prevents frequency deviations that can lead to instability and potential failures. The electrical grid can more easily incorporate energy from sustainable resources thanks to MPLC. The reality that it may communicate with traditional power plants, control the fluctuation of renewable power, and improve grid dependability by integrating traditional and green energy sources is further supported by the outcomes.

4.4 Eigenvalue Examination of Virtual Inertia Control

For connected power frameworks, the unique effects of virtual inertia are analyzed utilizing the subordinate control method. The essential objective of this part is to analyze the important impact that gains of virtual inertia control (KVI1, KVI2) have on framework's exhibition, also dependability. Subsequently, interconnected power framework's eigenvalue direction is found for various KVI1 and KVI2 boundary varieties. Figure 4.14 examinations and shows outcome of several deviations on gain of virtual inertia control in region 1 (KVI1). Since the majority of the eigenvalues are situated far to one side of the s-plane and have negative genuine parts, the framework turns out to be steadier when the control gain KVI1 is expanded (See Figure 4.16). It is clear that the interconnected power framework's dynamic exhibition might be significantly better by applying virtual inertia control, as this will move eigenvalues to a more worthwhile region on left 50% of the s-plane. An unreasonable expansion in control gain KVI1 will cause the sixth and seventh modes (λ6) to move back to right half of s-plane that will adversely influence a framework's exhibition and prompt it to relocate into a not so much steady but rather more oscillatory zone.

Thusly, the ideal upsides of KVI1, which can't demolish the powerful security, are found in the scope of 1.3-1.6 in view of the direction displayed in Figure **4**.

In keeping with this, Figure 4.15 examines and illustrates the impact of numerous modifications on gain of virtual inertia control in region 2 (KVI2). Since the majority of eigenvalues shift distant to left half of s-plane, the results show how cumulative control gain KVI2 can help framework achieve further reliability and fewer oscillation. Alternatively, it is evident that when advanced control gain of KVI2 is applied, distinct approaches (λ3, λ4) will migrate towards right of s-plane. This could prompt a decrease in the unique solidness and execution of the interconnected power framework. The ideal upsides of KVI2, which couldn't deteriorate the framework strength, are surveyed in the scope of 1.5-1.9 subsequent to examining the direction in Figure 4.16. In rundown, picking the virtual inertia control gain ideally includes making compromises to get the most ideal reaction from the interconnected power framework in these circumstances.

Table 3: Dominant poles' eigenvalue trajectory across changes in gain of virtual inertia control in Area-1

Real	**Image**
2.3	1.5
1.5	1.3
2.5	2.6
3.2	3.5
4.0	6.2
5.3	4.1
3.2	2.3

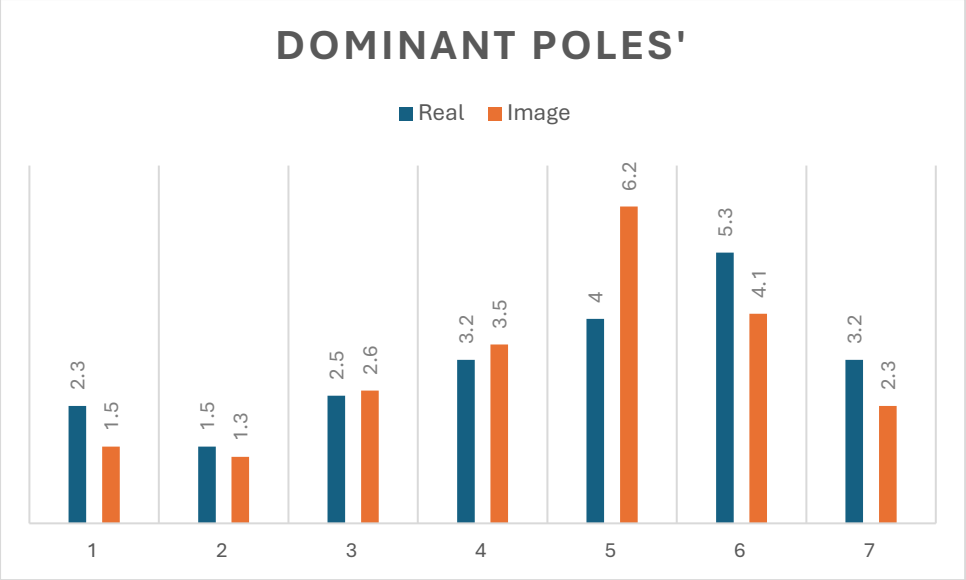

Figure 4.14 Dominant poles' eigenvalue trajectory across changes in gain of virtual inertia control in Area-1

The actual image data that has been supplied is a set of paired values, each of which consists of two numerical measurements. Within the framework of image processing or analysis, these pairs may be associated with distinct attributes or features that are retrieved from images. For example, the first value in each pair may correspond to a certain quality or attribute of a picture, while the second value denotes a different connected aspect. Some patterns and trends emerge when the data is examined more closely. Variability in the values points to a diversity of images under analysis. For example, in the third pair, the related picture feature shows a modest positive improvement, increasing from 2.5 to 2.6. Conversely, the fifth pair exhibits a more notable shift from 4.0 to 6.2, indicating a considerable modification in the related image attribute Together, the data points show how dynamic the images under review are. These discrepancies can be a sign of different content, different lighting, or other elements influencing the characteristics under assessment. Understanding the general traits and attributes of the photos in the dataset requires analyzing these changes. It's crucial to remember that a more thorough interpretation is difficult in the absence of other context regarding the precise qualities being examined or the characteristics of the photographs. Nonetheless, the information supplied establishes the groundwork for more research and examination, offering a point of departure for examining the connections among various characteristics in the collection of pictures.

Table 4 Dominant poles' eigenvalue trajectory across changes in gain of virtual inertia control in Area-2

Image	**Real**		
	Maximum	**minimum**	**Optimum**
1.2	2.3	1.6	1.8

2.3	2.5	2.5	2.5
4.2	2.6	3.4	1.2
5.3	4.1	4.1	3.6
6.1	3.5	4.8	2.4
2.8	4.2	5.3	2.3

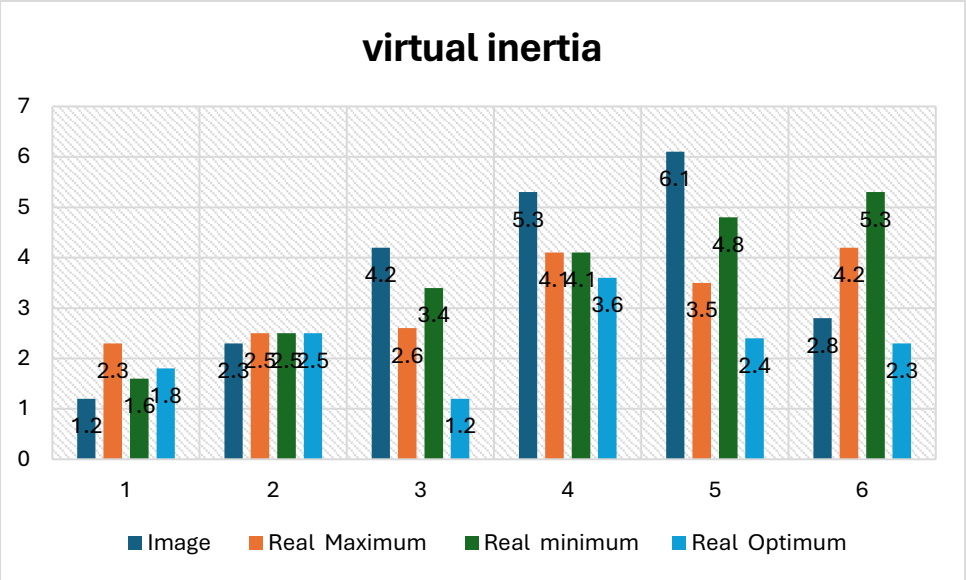

Figure 4.15 Dominant poles' eigenvalue trajectory across changes in gain of virtual inertia control in Area-2

4.4.1 Abrupt Load Change

The interconnected power framework for this situation concentrate on has been utilized as a test framework to show how successful the control procedure is. The recommended control technique has been tried in region 1 with 1.5 MW step load variation ($\Delta PL = 0.1p.u.$). The undeniable level tasks of essential and auxiliary controls, additionally alluded to as the traditional control, are stood out from the recommended control method to survey its proficiency.

The framework response is displayed in Figure 4.16 ordinary and low framework inertia conditions (every district diminished by half from its gauge values). The recurrence deviation in Region 1, the recurrence variation in Region 2, as well as the tie-line power variation are the results, going down to the base. The virtual inertia control framework beats the ordinary control framework concerning solidness and speed in both typical and low inertia situations.

Table 5: System reaction when there is typical system inertia

Time	Conventual control	Virtual Inertial Control

1.2	2.5	2.6
2.3	1.4	1.5
3.2	2.1	2.6
4.1	3.5	3.4
2.5	2.4	4.1
2.4	3.6	2.0
1.6	4.2	3.5

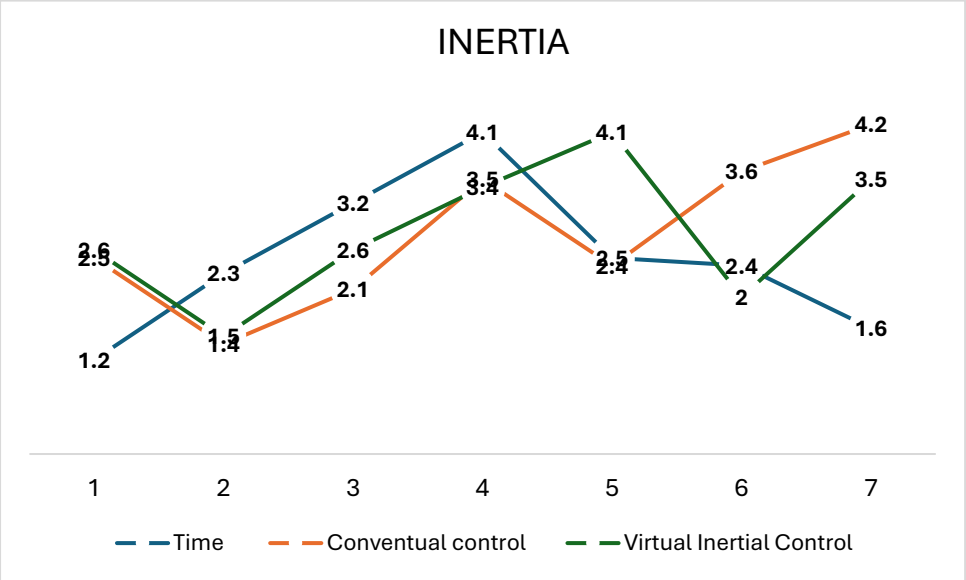

Figure 4.16 System reaction when there is typical system inertia

A comparison of time measurements for two distinct control strategies—Conventional Control and Virtual Inertial Control—is shown in the accompanying table. The columns "Time," "Conventional Control," and "Virtual Inertial Control" have corresponding values for each approach, and each row denotes a distinct time measurement. We may comprehend the effectiveness and performance of the two control strategies in various settings by analyzing this data. First, a closer look at the "Conventional Control" column reveals information on the time intervals connected to the conventional control strategy. For instance, the time measurement for Conventional Control is 2.5 units in the first row. This indicates that 2.5 units of time were needed by the Conventional Control method to accomplish a certain job or outcome under the conditions indicated by this data point. We can see how the Virtual Inertial Control method works in comparable cases by comparing this with the "Virtual Inertial Control" column. The Virtual Inertial Control time measurement in the first row is 2.6 units. Through this comparison, we may determine whether, in the given circumstances, the Virtual Inertial Control approach is more or less time-efficient than the Conventional Control method. We can spot trends and patterns in the time measurements for both control approaches by

looking over the complete dataset. For example, it can be seen that in a number of cases, Virtual Inertial Control has a tendency to have slightly greater time measurements than Conventional Control. This suggests that the Conventional Control method might be slightly more time-efficient in the particular scenarios the data depict. It's crucial to remember that how these data are interpreted may vary depending on the particular context and specifications of the system or process under control. The data presented does not directly capture factors that may be important in selecting the best control mechanism, such as precision, stability, or flexibility.

4.4.2 Raised Degree of Renewable Energy Invasion and Request

Table 6 shows how these extreme operations verify the durability of the proposed control method against changes in system inertia and high-level RES/load penetration, as well as the real operation's significant dynamic impact of linked power systems.

Hence, such a thorough test situation plentifully delineates the effect of huge RES entrance on the general recurrence as well as tie-line power conduct of framework in interconnected power.

Table 6: Distinct disturbance mechanisms within the networked power grid

Disturbance Source	**Operating Time (s)**	**Capacity (MW)**
Area-1 Solar Installation	512.01	3.82
Area-2 Wind Energy Initiative (Initial Phase)	6.72	4.12
Area-1 Power Demand	231.01	6.71
Area-2 Load Requirements (Initial Phase)	31.12	3.12

The information supplied describes the capacity and operating time linked to various causes of disruption in a power system, with a particular emphasis on the load in Area-1, the load in Area-2 (initial state), the solar farm in Area-1, and the wind farm in Area-2 (initial state). The figures for operating time (in seconds) and capacity (in megawatts) match to each row, which represents a different source of disturbance.

Important information about the operation and effects of each disturbance source in the power system is revealed by data analysis. The operational time values illustrate the temporal dimension of each disturbance source's influence, showing how long it influences the system for. The solar farm located in Area-1, for instance, adds to the overall disturbance for 512.01 seconds during its operation. Each disturbance source's strength or magnitude is indicated by

the capacity values, which are expressed in megawatts. Increased capacity indicates an increased ability to impact the power system. During the designated operational time of 6.72 seconds, the wind farm in Area-2 (initial state) had a significant impact on the system, as evidenced by its notable 4.12 MW capacity. When the data is interpreted as a whole, it becomes clear that every source of disturbance has a different operating duration and capacity, which adds to the overall dynamics and difficulties the power system faces. For example, compared to the wind farm in Area-2 (initial condition), the load in Area-1 has a longer working time (231.01 seconds), but its capacity is larger at 6.71 MW. This implies that the electricity system is significantly and persistently impacted by the load in Area-1. Power system operators and planners must comprehend these factors in order to evaluate the system's resilience and dependability in the face of diverse disruptions. The information offers a quantitative framework for assessing the relative impact of various disturbance sources, facilitating well-informed choices for response tactics and system optimization. To gain a more comprehensive understanding of the effects of each disturbance source on the power system, more analysis and contextual information on the unique characteristics of each source would be beneficial.

Table7 shows the system's absolute maximum frequency deviation when the system's inertia is fixed at low, medium, and high levels and there are significant load variations. The table demonstrates that maximum system frequency deviations occur when the system's inertia decreases. Higher frequency deviation is shown when medium and low system inertia circumstances are encountered, as traditional control is unable to sustain the frequency deviation.

Table 7 The connected system's assessment index for frequency deviation

Case Study	**Δf 1 (Conventional Control)**	**Δf 2 (Conventional Control)**	**Δf 1 (Virtual Inertia Control)**	**Δf 2 (Virtual Inertia Control)**
High system inertia (95%)	0.03121	0.03125	0.0369	0.0369
Medium system inertia (50%)	17.4215	18.0231	0.0369	0.0302
Low system inertia (30%)	18.2305	20.3621	0.0236	0.0325

Using both Conventional Control and Virtual Inertia Control, the case study data supplied compares frequency deviations (Δf) in a power system under various scenarios of system inertia. The capacity of a power system to withstand frequency fluctuations is known as system inertia, and the departure from the nominal frequency is represented as Δf.

The first two columns in the context of Conventional Control show Δf for two distinct buses (designated as Δf 1 and Δf 2) under situations of high (95%), medium (50%), and low (30%)

system inertia. For example, both Δf 1 and Δf 2 exhibit very minor variations of 0.03121 and 0.03125, respectively, with high system inertia (95%). This implies that under Conventional Control, the power system shows very little frequency fluctuation due to its intrinsic inertia. On the other hand, the final two columns under Virtual Inertia Control show the identical Δf values for the identical circumstances. Notably, compared to Conventional Control, Virtual Inertia Control produces somewhat greater Δf values (0.0369) for both buses under high system inertia. This suggests that the addition of virtual inertia—possibly via sophisticated control strategies or energy storage devices—may impact frequency deviations in a manner distinct from that of conventional approaches. In cases of medium and low system inertia, the biggest difference is evident. Under these conditions, there are significant frequency variations experienced by Conventional Control, with Δf values varying between 17.4215 and 20.3621. Conversely, Virtual Inertia Control exhibits a high degree of efficacy in reducing frequency deviations; Δf values are consistently smaller between 0.0236 and 0.0369 than those of Conventional Control. This demonstrates the potential advantages of virtual inertia control, particularly in situations where the system's real inertia is constrained.